

# Micromagnetic calculations of ferromagnetic resonance in submicron ferromagnetic particles

S. Jung, J. B. Ketterson, and V. Chandrasekhar

*Department of Physics and Astronomy, Northwestern University, Evanston, Illinois 60208*

(Received 30 May 2002; published 8 October 2002)

Micromagnetic simulations of the ferromagnetic resonance (FMR) spectrum of submicron circular ferromagnetic particles show a number of well-defined absorption peaks as a function of the applied dc magnetic field. In addition to a single large peak due to the uniform mode of precession, smaller peaks are observed on both sides of the uniform mode peak, corresponding to nonuniform or spin-wave modes of precession. The positions of these peaks are a function of particle size. Simulations of the FMR spectrum with and without exchange interactions show that the primary contribution to the energy of the spin-wave modes with absorption peaks at magnetic fields smaller than the uniform mode peak is from exchange interactions, whereas the primary contribution to the energy of the spin-wave modes above the uniform resonance mode arises from dipolar interactions, although all spin-wave modes have some contributions from both types of interactions.

DOI: 10.1103/PhysRevB.66.132405

PACS number(s): 75.30.Ds, 76.50.+g, 73.21.-b

## I. INTRODUCTION

Arrays of small, submicron ferromagnetic particles are becoming of increasing interest as potential candidates for magnetic storage. The idea is that each ferromagnetic particle corresponds to one bit of information, according to its direction of magnetization. Writing a bit of information implies changing the direction of magnetization of the particle. For high-speed applications, the mechanism of magnetization reversal is important. In smaller, single-domain particles, this reversal might occur by coherent rotation of the magnetization.<sup>1</sup> In larger particles, the rotation may be nonuniform, through the generation and propagation of spin waves. In order to minimize the reversal time, it is important to understand the nature of the spin-wave modes and their dependence on particle shape, size and material parameters.

Experimentally, ferromagnetic resonance (FMR) is a powerful means of probing the dynamics of magnetization in ferromagnetic films.<sup>2</sup> In the presence of an external magnetic field  $H_0$ , the magnetization  $\mathbf{M}$  of a ferromagnet precesses according to the Landau-Lifschitz equation<sup>1</sup>

$$\frac{d\mathbf{M}}{dt} = -\gamma\mathbf{M}\times\mathbf{H}_{\text{eff}} - \frac{\gamma\alpha}{M_s}\mathbf{M}\times(\mathbf{M}\times\mathbf{H}_{\text{eff}}), \quad (1)$$

where  $\gamma = ge/2mc$  the gyromagnetic ratio ( $g$  being the Landé factor and  $m$  the mass of the electron),  $\mathbf{H}_{\text{eff}}$  the effective local field,  $M_s$  the saturation magnetization, and  $\alpha$  the damping constant. This causes a precession of the moment about the direction of the field at a frequency  $\omega_0$ . For an ellipsoidal ferromagnet body (with a uniform magnetization),  $\omega_0$  is given by the Kittel equation<sup>3</sup>

$$\omega_0^2 = \gamma^2[H + (N_x - N_z)M][H + (N_y - N_z)M], \quad (2)$$

where the  $N_x$ ,  $N_y$ , and  $N_z$  are the demagnetization factors along the  $x$ ,  $y$ , and  $z$  directions that satisfy the relation  $N_x + N_y + N_z = 4\pi$ , with the  $z$  direction defined by the direction of the external field  $H$ , which is applied along one of the principal axes of the ellipsoid. An ac magnetic field  $H_{\text{ac}}$  at this resonant frequency applied perpendicular to  $H$  will couple to a uniform precession of  $M$  about the direction of  $H$ ,

resulting in absorption of energy from the ac field. For example, for a uniform sphere with  $N_x = N_y = N_z$ ,  $\omega_0 = \gamma H$ , while for a thin film with the external magnetic field aligned perpendicular to the film plane,  $N_x = N_y = 0$ ,  $N_z = 4\pi$ . This means that the resonance is shifted to higher values of external magnetic field,  $\omega_0 = \gamma(H - 4\pi M)$ , due to demagnetization effects in the film.

In addition to the uniform mode, the external ac field may also couple to nonuniform or spin-wave modes of precession. Contributions to the energy of these modes arise from a combination of exchange and dipolar interactions. Kittel considered case where the primary additional contribution arises from exchange interactions.<sup>4</sup> In his model, the spin-wave modes lead to additional resonances at frequencies given by  $\omega_p = \omega_0 + Dk_p^2$ . Here  $D$  is a constant that depends on the exchange interaction in the ferromagnet, and  $k_p$  is the wave vector of the spin-wave mode, which is quantized due to pinning of the moments at the sample surface. For example, for a thin film of thickness  $d$ ,  $k_p = (2p - 1)\pi/d$ , where  $p = 1, 2, 3, \dots$ . Since the frequency is always higher than that of the uniform mode, the presence of exchange spin waves lead to multiple peaks in the FMR spectrum at external magnetic fields less than the magnetic field  $H_0$ , corresponding to the uniform mode, with the spacing of these peaks being determined by the thickness of the film.<sup>5</sup>

Exchange interaction contributions to the spin wave modes are more important at smaller length scales. For larger ferromagnetic samples, dipolar contributions to the energy of the spin-waves may be dominant.<sup>6</sup> In contrast to the exchange modes, the frequencies of these magnetostatic or Walker modes are expected to be essentially independent of the size of the ferromagnet, and may be lower or higher than the frequency of the uniform mode, leading to peaks in the FMR spectrum at external field values both above and below  $H_0$ .

In the intermediate size regime of interest to us here, both exchange and dipolar interactions make contributions to the energies of the spin-wave modes. Unfortunately, unlike the limiting cases discussed above, analytical solutions for the frequencies of the spin-wave modes are difficult to obtain in this regime, and one must resort to numerical techniques.

Numerical simulations on such systems show that the FMR peaks corresponding to the spin-wave modes can be both above and below the uniform mode peak, but the resonance frequencies depend in a complicated way on the size and shape of the ferromagnetic particle.<sup>7,8</sup>

In this Brief Report, we report on our techniques for simulating the ferromagnetic resonance response of single ferromagnetic particles. These micromagnetic simulations were motivated by recent experiments on FMR in arrays of ferromagnetic nanoparticles.<sup>9</sup> We find that the FMR spectrum of a small ferromagnetic particle shows a number of peaks both above and below the position  $H_0$  of the uniform mode peak. The position of the peaks is a function of the size of the particles. Although the energy of the corresponding spin-wave modes have contributions from both exchange and dipolar interactions, by varying the exchange stiffness parameter in the simulations, we determine that the spin-wave modes corresponding to resonance peaks at field values  $H < H_0$  have contributions mainly from exchange interactions, while those resonance peaks occurring at field values  $H > H_0$  have contributions primarily from dipolar interactions.

## II. DETAILS OF CALCULATION

The simulations were performed by numerically integrating the Landau-Lifschitz equation [Eq. (1)], using the public domain OOMMF micromagnetic solver.<sup>10</sup> This program uses a regular two-dimensional (2D) grid of squares with a cell size  $a$ , with the magnetization in the center of each cell being three-dimensional (3D), and assumes Neumann boundary conditions (further details of the program can be found in Ref. 10). Although the grid is 2D, the program does assume a finite thickness of the film (85 nm in our calculations): the finite thickness of the film affects the results through the demagnetization factor, as we shall see later. For FMR, a static (dc) field and an ac field are required. The static (dc) field was varied from 0 to 5000 Oe at intervals of 10 Oe. At each value of the dc field, the local magnetization of each cell was first aligned in the direction of the external field. An ac field  $H_{ac}$  of the form

$$H_{ac} = (1 - e^{-\lambda t}) H_{ac0} \cos(\omega t) \quad (3)$$

was then applied perpendicular to the dc field, where the frequency of the ac field,  $f = \omega/2\pi = 9.37$  GHz, was chosen to match the experiments.<sup>9</sup> Both the dc field and the ac field were applied in the plane of the particle. To be definite, we shall take the direction of the dc field to be in the  $z$  direction, and the direction of the ac field to be in the  $x$  direction. The factor  $(1 - e^{-\lambda t})$  in Eq. (3) was introduced to ensure adiabatic turn-on of the ac field;  $\lambda$  was chosen so that the ac field grew over the first few cycles ( $\lambda \approx f$ ). To determine the FMR spectrum, the Fourier transform of the average magnetization in the  $x$  direction was calculated. Transient effects were eliminated by ignoring the response in the first 20–50 cycles of the ac field, and averaging only over the last few hundred cycles.

Figure 1 shows the calculated absorption spectrum for a circular particle of diameter  $d = 0.5 \mu\text{m}$  as a function of cell size. The magnetic parameters for the calculation are those

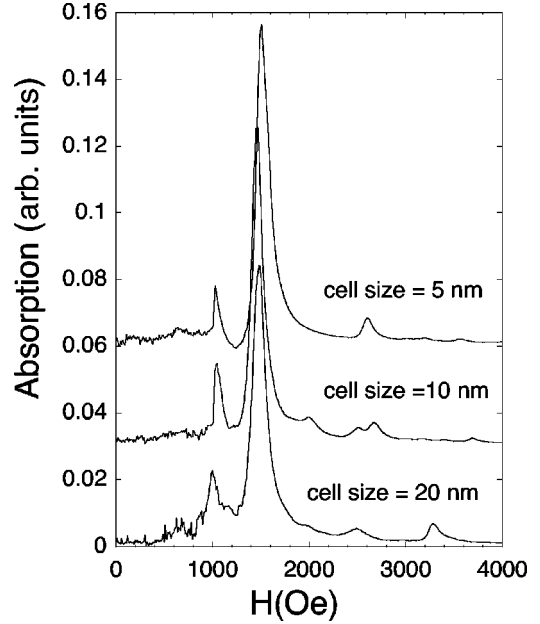


FIG. 1. Calculated FMR spectra for a  $d = 0.5 \mu\text{m}$  ferromagnetic particle, using three different cell sizes: 5, 10, and 20 nm. The other parameters in the calculations are those usually taken for Permalloy, i.e., saturation magnetization  $4\pi M_s = 1.064 \times 10^4$  G, exchange stiffness  $A = 1.3 \times 10^{-6}$  ergs/cm, and damping constant  $\alpha = 0.05$ . The curves have been offset by 0.03 along the ordinate for clarity.

usually taken for Permalloy, with saturation magnetization  $4\pi M_s = 1.064 \times 10^4$  G, exchange stiffness  $A = 1.3 \times 10^{-6}$  ergs/cm, and damping constant  $\alpha = 0.05$ . In all three curves, two major peaks are seen. The largest central peak at  $H_0 \approx 1500$  Oe corresponds to the uniform mode of precession. A second peak is observed below the uniform resonance mode at an external field of  $H \approx 1000$  Oe. The position of this peak does not depend on the cell size used to calculate the FMR spectrum. In contrast, the position and amplitude of the peaks at external field values larger than  $H_0$  appear to strongly depend on the cell size. Ideally, of course, one should use a cell size as small as possible in order to model real ferromagnets; realistically, one is restricted by computing power, since the smaller the cell size, the longer the calculation time. Our calculations show that there is not an appreciable difference between a cell size of 4 nm and a cell size of 5 nm; consequently, we have used a cell size of 5 nm in most of our calculations.

Some indication of the various contributions to the energy of the spin-wave modes corresponding to the peaks seen the FMR spectrum can be seen by varying the parameters in the calculation, in particular the exchange constant  $A$ . Figure 2(a) shows the absorption spectrum for a  $d = 0.5 \mu\text{m}$  circular Permalloy particle with a cell size of 5 nm and parameters as discussed above (saturation magnetization  $4\pi M_s = 1.064 \times 10^4$  G, exchange stiffness  $A = 1.3 \times 10^{-6}$  ergs/cm and damping constant  $\alpha = 0.05$ ). Figure 2(b) shows the results of a second calculation, identical in all respects to the first, except that the exchange stiffness constant  $A$  has been set to 0. The major difference between the two curves is the absence of the peak at  $H \approx 1000$  Oe in the second curve, showing

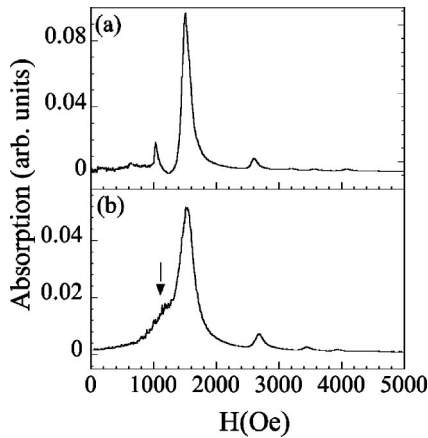


FIG. 2. (a) Calculated FMR spectrum for a  $d=0.5 \mu\text{m}$  ferro-magnetic particle, with a cell size of 5 nm, and other parameters as in Fig. 1 (saturation magnetization  $4\pi M_s=1.064\times 10^4$  G, exchange stiffness  $A=1.3\times 10^{-6}$  ergs/cm, and damping constant  $\alpha=0.05$ ). (b) Same as in (a), except that the exchange constant  $A=0$ .

clearly that this peak has its primary contribution from exchange interactions. We shall consequently call this peak the “exchange” peak, although experiments show that it also has contributions to its energy from dipolar interactions.<sup>9</sup> The peaks above  $H_0$  are not substantially affected, showing that the primary contribution to their energy comes not from exchange interactions but dipolar interactions; however, their positions are shifted slightly, indicating that they have at least a small contribution to their energy from exchange interactions. Note also the presence of a small shoulder below  $H_0$  at around  $H\approx 1200$  Oe (denoted by an arrow in the figure). This is a dipolar mode; as is known from the work of Walker,<sup>6</sup> these modes can occur both above and below the uniform mode.

According to Kittel’s theory, the offsets of the exchange mode peaks from the uniform mode peak are given by the quantization of the spin wave vectors  $k_p$ , which in turn is determined by the dimensions of the ferromagnet.<sup>4,5,11</sup> As the dimensions of the ferromagnet decrease, the field difference between exchange mode peaks and the uniform mode peak should increase. Although Kittel’s analytical calculation can only be performed for specific simple geometries, the numerical calculations show similar behavior on sample size. Figure 3(a) shows numerical calculations for circular Permalloy dots of five different diameters  $d$ . In this calculation, a cell size of 10 nm was used, with all the other parameters being identical to the calculations of Fig. 1. As expected, all peaks shift down in magnetic field as the particle diameter is increased; this is most clearly seen for the uniform mode peak. This is due to demagnetization effects associated with the size of the particle, since it is assumed to have a finite thickness. However, the difference in magnetic field between the position of the uniform mode peak and the peak corresponding to the exchange mode just below it also increases. Figure 3(b) shows the position of the uniform mode peak, the position of the exchange mode peak, and the difference in position between the two peaks as a function of sample size.

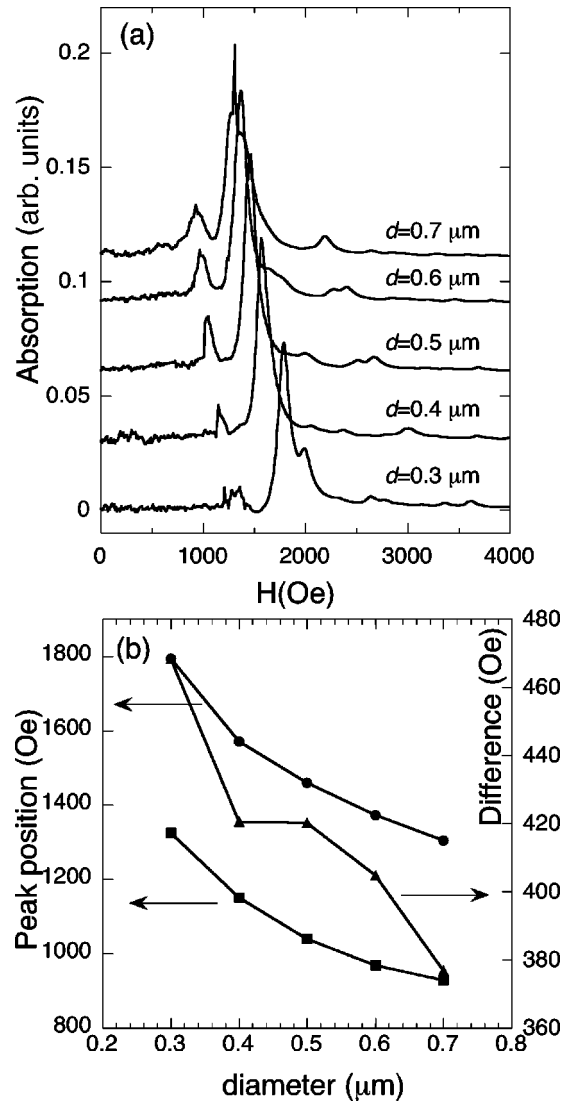


FIG. 3. (a) Calculated FMR spectra with a cell size of 10 nm, for five different particle diameters. The other parameters are the same as for Fig. 1. The curves have been offset by 0.03 along the ordinate for clarity. (b) Magnetic field position of the uniform mode peak (filled circles), “exchange” mode peak (filled squares), and difference between the two peaks (filled triangles).

The position of both the uniform and the exchange mode peaks varies as a power law in the diameter (the best fit is  $\approx d^{-0.4}$ ); however, the difference in position between the two peaks also decreases with increasing particle diameter. This is in qualitative agreement with the predictions of Kittel’s model.

Similar behavior is also seen for the positions of the dipolar modes; however, the behavior appears much more complex due to the multiplicity of peaks, so that it is difficult to trace the evolution of peak position with particle size. Nevertheless, one can still discern a pattern to the variation of the peak position with particle size, which is stronger than the simple shift due to demagnetization factors. The peaks appear primarily at values of magnetic field larger than  $H_0$ , although some of the resonances occur below  $H_0$  as we noted above, and even on top of the uniform mode peak, as

is seen in the data for the  $d=0.7\ \mu\text{m}$  particle. (Indeed, the uniform mode peak can be thought of as a dipolar spin-wave mode peak.) For example, in the curve for the  $d=0.6\ \mu\text{m}$  particle, there is a double peak at  $H\approx 2300\ \text{Oe}$ , which has moved up to  $H\approx 2600\ \text{Oe}$  in the curve for the  $d=0.5\ \mu\text{m}$  particle. Although they are not so prominent, smaller resonance peaks can also be observed below  $H_0$ ; an example is the small hump at  $H\approx 1400\ \text{Oe}$  in the  $d=0.4\ \mu\text{m}$  curve. As we have noted above, these resonances observed at fields above and below  $H_0$  are associated primarily with spin-wave modes where the primary contribution to the energy is from dipolar interactions. Further evidence that dipolar interactions provide the primary contribution to the energy of these modes comes from experiment, where it is found that the amplitude and position of these FMR resonance peaks in arrays of magnetic nanoparticles are strongly affected by the interparticle dipolar coupling.<sup>9</sup> Note, however, that unlike the predictions for dipolar-coupled Walker modes,<sup>6</sup> the energies of these modes are not independent of sample size, since the resonance peaks shift with as the particle size is changed. We stress again that the notation “exchange” and “dipolar” are more convenient labels than accurate descriptions of the nature of the spin-wave modes, since in small ferromagnetic

particles, they all involve a coupling of exchange and dipolar interactions.

In summary, we have performed numerical calculations of the FMR absorption spectrum of circular ferromagnetic particles, where analytical calculations of the spin-wave modes is not feasible. In addition to the resonance peak corresponding to the uniform mode, the FMR spectrum shows numerous peaks both above and below the uniform mode peak. The position of all peaks is a function of particle size. By varying parameters, it is found that the most prominent resonance peak below the uniform mode peak corresponds to a spin-wave mode whose energy arises primarily from an exchange interactions, while the spin-wave modes associated with other peaks above and below the uniform mode peak are primarily dipolar in nature.

### ACKNOWLEDGMENTS

We thank Anupam Garg for useful discussions, and Robert Tilden for use of computer facilities. This work was supported by the Army Research Office through Grant No. DAAD19-99-1-0339, and by the David and Lucile Packard Foundation.

<sup>1</sup>See, for example, A. Aharoni, *Introduction to the Theory of Ferromagnetism* (Oxford University Press, New York, 1996).

<sup>2</sup>See, for example, *Ultrathin Magnetic Structures II*, edited by B. Heinrich and J. A. C. Bland (Springer, Berlin, 1994).

<sup>3</sup>C. Kittel, *Introduction to Solid State Physics, 7th Edition* (John Wiley and Sons, New York, 1996).

<sup>4</sup>C. Kittel, *Phys. Rev.* **110**, 1295 (1958).

<sup>5</sup>M. H. Seavey, Jr. and P. E. Tannenwald, *Phys. Rev. Lett.* **1**, 168 (1958).

<sup>6</sup>L. R. Walker, *Phys. Rev.* **105**, 390 (1957).

<sup>7</sup>P. A. Voltairas, D. I. Fotiadis, and C. V. Massalas, *J. Appl. Phys.* **88**, 374 (2000).

<sup>8</sup>R. Arias and D. L. Mills, *Phys. Rev. B* **63**, 134439 (2001).

<sup>9</sup>S. Jung, D. Watkins, L. DeLong, J. B. Ketterson, and V. Chandrasekhar, *Phys. Rev. B* (to be published).

<sup>10</sup>M. J. Donahue and D. G. Porter, *OOMMF User's Guide, Version 1.0*, Interagency Report NISTIR No. 6376, National Institute of Standards and Technology, Gaithersburg, MD (1999); URL: <http://math.nist.gov/oommf>. For a more detailed description of some of the numerical techniques, please see D. V. Berkov, K. Ramstöck, and A. Hubert, *Phys. Status Solidi A* **137**, 207 (1993).

<sup>11</sup>Ph. Toneguzzo, O. Acher, G. Viau, F. Fiévet-Vincent, and F. Fiévet, *J. Appl. Phys.* **81**, 5546 (1997).